JMEPEG (2015) 24:3038–3048
DOI: 10.1007/s11665-015-1574-2

1059-9495/$19.00

X-ray Diffraction Investigations of Shape Memory NiTi Wire

Mohammad Honarvar, Bardia Konh, Tarun K. Podder, Adam P. Dicker, Yan Yu, and Parsaoran Hutapea

(Submitted December 10, 2014; in revised form May 29, 2015; published online June 18, 2015)

Outstanding properties of nitinol, known as shape memory and superelasticity, make them suitable alternatives in several biomedical, aerospace, and civil applications. For instance, nitinol wires have been used as the actuator components in many innovative medical devices aiming to make surgical tasks less invasive and more efficient. In most of these applications, it is desired to have a consistent strain response of nitinol wires; therefore, it is necessary to investigate the internal phase transformations from microstructural point of view. In this study, the effect of influencing factors such as biased stress during thermal cycle, the maximum temperature wires experienced during heating part of thermal cycle, and also wire diameters on the amount of unrecovered strain occurred between the first and the second thermal cycles has been investigated. The generation of different phase compositions in the same thermomechanical condition for different wire diameters has been discussed using x-ray diffraction (XRD) method. The location and intensity of characteristic peaks were studied prior and after the loading cycles. It was observed that nitinol wires of diameters less than 0.19 mm exhibit unrecovered strain while heated to the range of 70-80 °C in a thermal cycle, whereas no unrecovered strain was found in wires with larger diameter. The observation was supported by the XRD patterns where the formation of R-phase instead of martensite was shown in wire diameters of less than 0.19 mm after cooling back to room temperature.

Keywords nitinol, one-way shape memory, phase identification, unrecovered strain, XRD

1. Introduction

Nitinol (NiTi) is near equiatomic intermetallic compound of Nickel and Titanium with approximate chemical composition of ≤ 49 Ni at.% ≤ 51. Nitinol is also considered as an alloy containing other chemicals elements as Co, Fe, V, Ta, Mo, and so on. Nitinol has two distinct crystal phases. One is known as austenite that exists at high temperatures with high symmetric crystal structure of type B2 also known as parent phase. The other phase is known as martensite that exists at low temperatures with lower symmetric crystal structure (orthorhombic or monoclinic). An intermediate R-phase with rhombohedral crystal structure may also form while cooling from austenite phase right before transforming to martensite (Ref 1). Shape memory behavior and superelasticity are the two outstanding properties of nitinol that can produce large cyclic elastic strain without causing plastic deformation. These properties make nitinol a good alternative for different applications such as biomedical devices, construction structures, mechanical engines, and aerospace engineering (Ref 2). For instance, one innovative medical device was proposed in the research performed by Hutapea et al. (Ref 3-11) where the actuation capabilities of nitinol wires were utilized to activate a prostate brachytherapy needle. The actuation is due to nitinol's high power to volume ratio and their ability to produce high recoverable strain and stress with small wire diameter. However, under certain ranges of stresses and temperatures, nitinol wires exhibit unrecovered strain between first and second thermal cycles (Ref 5, 11-14). Therefore, for cyclic repetitive applications, it is important to study the strain behavior of nitinol wires.

Based on the amount of biased stress along the wire during thermal cycle, the transformation of austenite to twinned or detwinned martensite during cooling can happen. If the amount of stress is in the range of critical stress then, detwinned martensite forms which causes full strain recovery and negligible unrecovered strain otherwise, the twinned martensite with high value of unrecovered strain happens (Ref 15, 16). There are four characteristic temperatures known as A_s, A_f, M_s, and M_f, which represent the start and finish temperatures of austenite and martensite. Subscripts *s* and *f* represent the start and finish of transformation and *M* and *A* represent martensite and austenite, respectively. There are some critical stresses for the formation of martensite from the parent phase known as σ_{Ms}, σ_{Mf}, σ_{As}, and σ_{Af} (Ref 1). A minor change in chemical composition of nitinol can cause a noticeable change in mechanical behavior, transformation temperatures, and transformation stresses (Ref 17).

The direct and reverse phase transformation between austenite and martensite result in two outstanding behaviors, namely shape memory effect and superelasticity. Thermomechanical loadings, i.e., temperature and stress changes, are the major driving causes of the phase transformation in nitinol (Ref 18). The strain behavior of nitinol wires is greatly influenced by the loading conditions such as the biased stress and the maximum temperature during thermal cycles. In one-

Mohammad Honarvar, Bardia Konh and **Parsaoran Hutapea**, Department of Mechanical Engineering, Temple University, 1947 N 12th Street, Philadelphia, PA 19122; **Tarun K. Podder**, Department of Radiation Oncology, Case Western Reserve University, 11100 Euclid Avenue, Cleveland, OH 44106; and **Adam P. Dicker** and **Yan Yu**, Department of Radiation Oncology, Thomas Jefferson University, 111 S. 11th Street, Philadelphia, PA 19107. Contact e-mails: tuc74687@temple.edu and hutapea@temple.edu.

way shape memory, nitinol undergoes a large elastic strain during thermal cycles while being under sufficient amount of biased stress. This amount of biased stress is important basically to achieve a consistent strain response in cyclic thermomechanical loadings. This behavior is not being observed in two-way shape memory nitinol (Ref 12, 19, 20).

Honarvar et al. (Ref 13) have studied the dependencies of one-way shape memory nitinol on the critical stresses and the range of heating temperatures in thermal cycles for different wire diameters. In one-way shape memory, the complete strain cycle consists of the direct transformation from detwinned martensite to austenite (heating) and the reverse transformation back to detwinned martensite (cooling). The previous studies showed that the amount of biased stress should be in the range of the critical stress required to form detwinned martensite from twinned martensite (Ref 13, 21). For instance, the range of critical stress to avoid an unrecovered strain in the cooling cycle in 0.19 mm wire diameter was found 120 MPa (Ref 13).

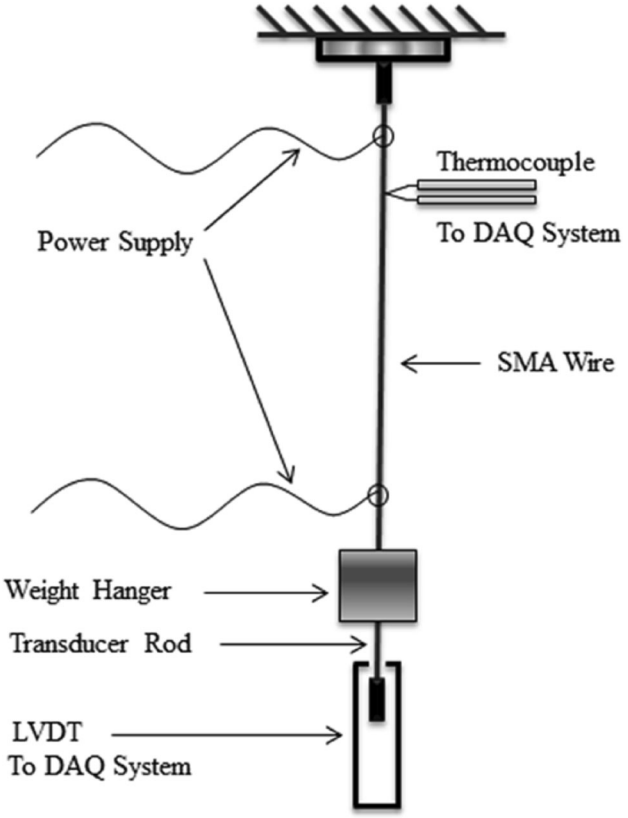

Fig. 1 A schematic picture of the constant stress test

Superelastic nitinol shows a large amount of strain, about 7%, under the application of stress at temperatures higher than A_f. By increasing the stress above the critical amount of formation of martensite (σ_M), a large strain plateau occurs due to the transformation of austenite to martensite (Ref 13). By decreasing the stress lower than this critical stress, the phase transformation from martensite to austenite occurs and cyclic strain happens in the nitinol microstructure (Ref 22, 23).

In the work performed by Honarvar et al. (Ref 13), it was observed that the unrecovered strain in the first loading-unloading cycle has a great influence on the total strain in the subsequent cycles. Moreover, a critical range of stress was found beyond which the unrecovered strain was negligible while the wires heated up to the range of 70-80 °C, depending on the wire diameters. The unrecovered strain of wire diameters smaller than 0.19 mm was found to be sensitive to the critical stress. On the other hand, for wire diameters bigger than 0.19 mm the connection between the unrecovered strain and the critical stress were not observed for the same range of heating temperature. The main reason for such a behavior was the generation of different phases prior and after the thermal cycles. An insufficient heat during heating process could be found as a reason for such a different behavior in larger diameters that ultimately caused different phases after cooling cycle. The normal heating temperatures for nitinol wires in their application, i.e., actuators for brachytherapy needles, were about 70-80 °C. Honarvar et al. (Ref 13) concluded that when

Table 2 DSC results for different nitinol wire diameters

Wire diameter, mm	M_f,°C	M_s, °C	A_s, °C	A_f, °C
0.15	−18	26	52	64
0.19	−33	15	42	75
0.24	−30	12	42	64
0.29	−32	15	37	67

Table 1 Wire preconditioning procedure and generated crystal structure prior to XRD test

Case No.	Wire diameter, mm	Heating cycle, °C	Cooling cycle (°C)	Mechanical treatment	Major phase state after conditioning
As-received	0.15, 0.19 0.24, 0.29	NA	NA	NA	Detwinned martensite
1	0.15, 0.19 0.24, 0.29	70-80 °C in CS	RT, CS	N.A	R-phase Detwinned martensite
2	0.15, 0.19 0.24, 0.29	120-130 °C in CS	RT, CS	NA	R-phase
3	0.15, 0.19 0.24, 0.29	70-80 °C in CS	RT in CS/−40 °C in CC	NA	Twinned martensite Detwinned martensite
4	0.15, 0.19 0.24, 0.29	70-80 °C in CS	R.T in CS/−40 °C in CC	5% Strain in UTT Negligible strain	Detwinned martensite

The crystal structure before conditioning is detwinned martensite
RT: Room Temperature, CS: Constant Stress, CC: Cooling Chamber, UTT: Uniaxial Tensile test

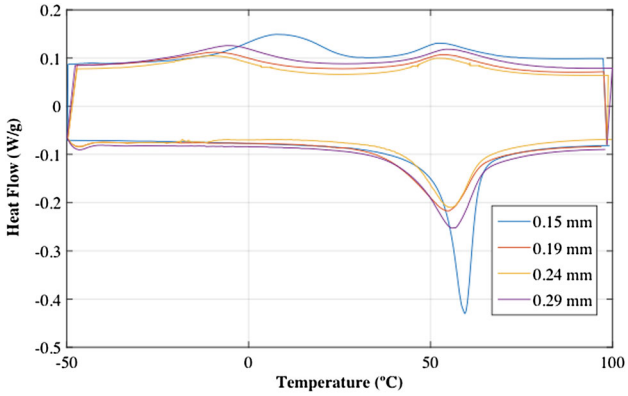

Fig. 2 DSC results of nitinol wires with diameters of 0.15, 0.19, 0.24, and 0.29 mm

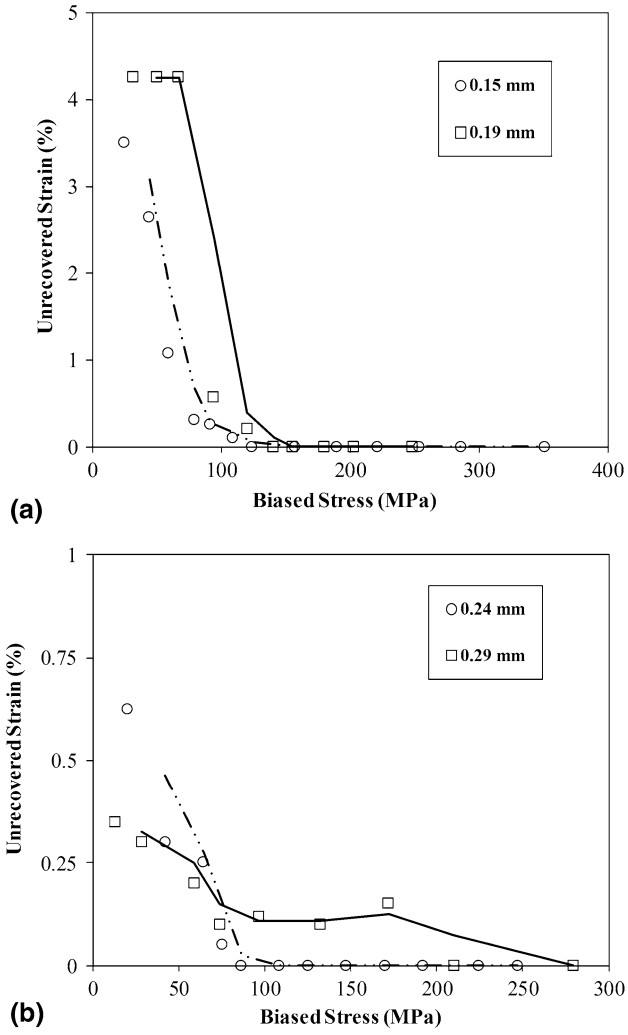

Fig. 3 Unrecovered strain versus biased stress for various wire diameters, (a) diameters less than 0.19 mm, (b) diameters bigger than 0.19 mm

thermal cycle was increased to 120-130 °C, an unexpected thermomechanical behavior such as low unrecovered strain could be observed for wires diameter larger than 0.19 mm. To prove their previous observation, x-ray diffraction (XRD) analyses have been performed in this study to capture the microstructure of nitinol wires at different thermomechanical loading conditions.

XRD is a suitable tool for determination of the crystallographic structures of materials. Performing XRD, the planes of atoms interfere constructively with x-rays and therefore diffraction occurs.

Conventional XRD and micro-XRD have been used advantageously to study phase composition of nitinol wires at room temperature (Ref 24-27). When the direct or reverse transformation between austenite to martensite occurs, XRD pattern shows different peaks at different angles with different intensities. During transformation new peaks appear while old peaks may disappear or split. Changes are dependent on the presence of austenite phase, the resolution of XRD data, and the orientation of the martensite to the diffractometer. Kheir et al. (Ref 28, 29) used XRD to identify phases before and after heat treatment of a superelastic nitinol. Thayer et al. (Ref 25) used XRD to obtain the phase transformation between austenite and martensite in a superelastic nitinol for orthodontics arch wires. They ranked the degree of transformation between austenite and martensite based on the intensity of austenite and martensite peaks. Iijima et al. (Ref 27) have used the micro-XRD technique to determine the phases in two superelastic nitinol orthodontic wires that demonstrated shape memory effect in the oral and super elastic behavior in vivo environments, respectively. For analyzing very small areas on orthodontic wires, micro-XRD is a highly convenient technique (since the diameter of analysis area is limited to 50 μm).

To identify the phases of nitinol samples with a bigger surface area, the conventional XRD technique is suggested (Ref 26, 27), although other techniques such as in situ synchrotron XRD have been used by Cai et al. (Ref 30) to perform texture evolution during nitinol martensite detwinning. In their studies, they reported the texture evaluation of a thermally martensitic wire and an austenitic wire during deformation. Their results revealed valuable information about wire orientation distribution and texture evolution. They demonstrated the martensite detwinning process with change in intensity of XRD patterns. In another work, Shen et al. (Ref 31) used XRD method to identify phases in the nitinol wires for rotary instruments. They achieved 3 major peaks for the (110), (200), and (211) atomic planes in austenite and couple of peaks for associated to martensite while they scanned their samples at 25 °C between 20° and 100°, 2θ angles.

Iijima et al. (Ref 32) investigated the mechanical properties and phase transformation of commercial superelastic nitinol orthodontic wires using DSC, three point bending test and micro-XRD. They showed the phase transformation between austenite and martensite when the temperature is decreased from 37 to 2 °C using micro-XRD method. They observed the major peak of (110) for austenite at the angle of 42.3° in non-loading condition. The (002) and (111) peaks for martensite phase appeared when the wires bent and the (110) peak for austenite were shifted about 0.3° to a high-angle side with a lower density. Similar methods were used in this study and the observations will be interpreted in the result section. Iijima et al. (Ref 32) have detected the phase changes in nitinol wires by the change in intensity and locations of major austenite and martensite peaks.

Iijima et al. (Ref 24) have also used XRD to study low-temperature phase transformation in nitinol orthodontic wires. In their study, the XRD measurements were performed in a Bragg-Brentano system. They attached 20 straight segments of

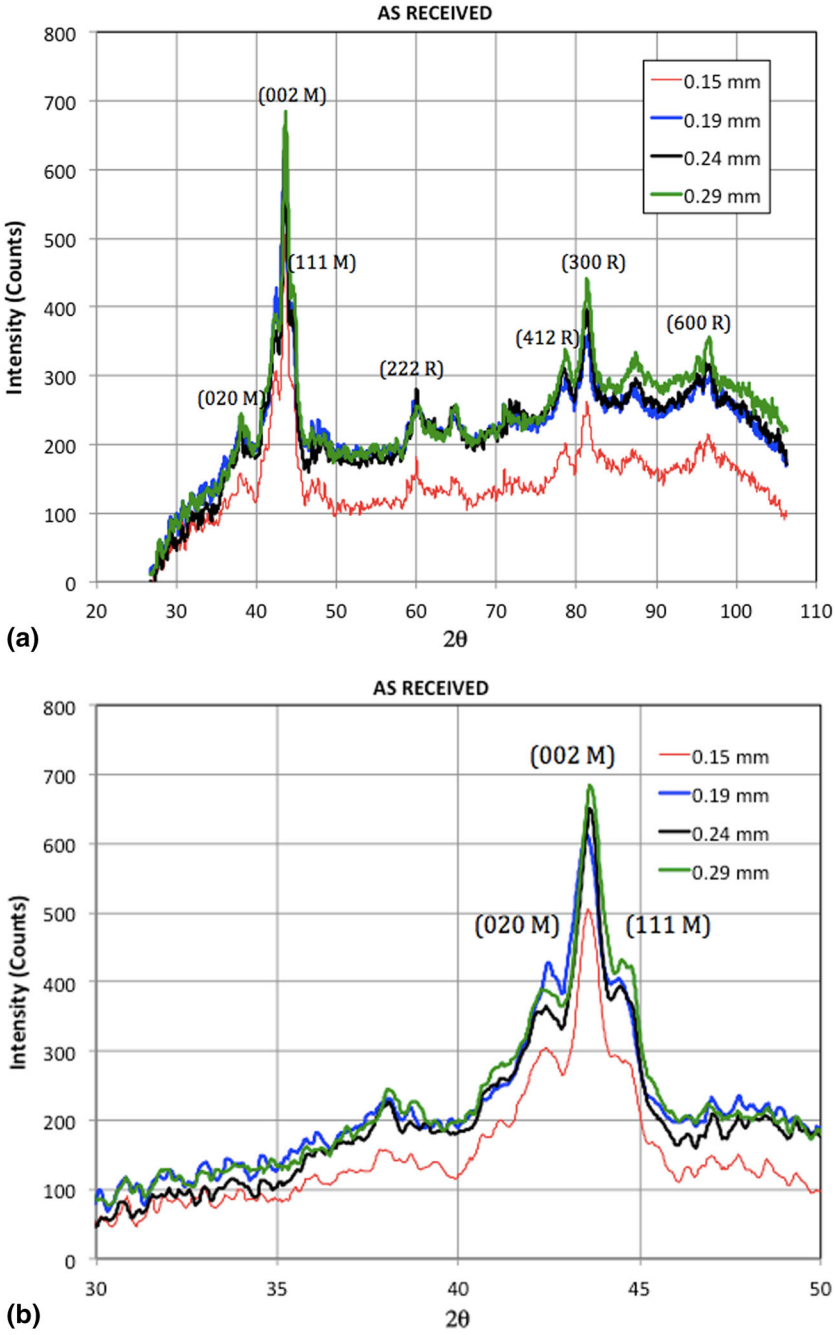

Fig. 4 (a) Complete XRD pattern of as-received wires; (b) XRD patterns between 30° and 50° 2θ angle

wire lying side by side to create a surface for x-ray scan and then analyzed over the 2θ angle ranged from 30° to 130°. They have obtained major characteristic peaks of different phases as (110) for austenite at the 2θ angle of 42.8. They obtained (002) peak for martensite at the 2θ of 43.92 also (112) and (300) for R-phase at 2θ angles of 42.2° and 42.7°, respectively. These peaks can be used as references for interpreting our XRD results in the current study. Kheir et al. (Ref 33) have used XRD method for analyzing the metallurgical structures of as-received and heat-treated stainless steel orthodontic wires.

In general, this work investigates the relationship between macroscopic strain behavior of nitinol wires and their phase compositions. The strain response of nitinol wires was studied using constant stress and uniaxial tensile tests while the microstructures were evaluated using the XRD method. Differential scanning calorimetry (DSC) tests were also performed to determine the phase transformation temperatures that are used to determine the temperature range of thermal cycle for the constant stress and the XRD tests. The detailed sample preparation procedure is explained in "Test Specimen Preparation" section under the methods section. The microstructure of nitinol wires at different thermomechanical conditions is described in the "X-ray Diffraction Test" section and the XRD analyses are presented in "Result and Discussions" section. Finally, the correlation of macroscopic strain response and the microstructure of the wires under each thermomechanical

condition are presented in the "Result and Discussions" section.

2. Experimental Method

2.1 Test Specimen Preparation

Nitinol wires of various diameters of 0.15, 0.19, 0.24, and 0.29 mm (obtained from Dynalloy, Inc., Tustin, CA, USA), commercially known as Flexinol, with A_f temperature of 70 °C at 172 MPa, were selected for our studies. The wires with a chemical composition of 50.5 at.% Nickel and 49.5 at.% Titanium and the length of 100 mm were discussed in this study. As-received flexinol wires have detwinned martensite crystal structure. They were pre-strained to 5% and tested and spooled to 104 MPa by the manufacturer before shipping. This amount of strain will be recovered during heating to austenite in one-way shape memory behavior. The transformation temperatures of these wires were measured by using the DSC instrument 2920 (TA Instrument, New Castle, DE, USA). In the DSC test, wire samples were heated to 120 °C at a constant rate of 10 °C/min and then cooled down to −100 °C. Nitrogen was used for both the cover and the purge gas.

In order to investigate the effect of microstructure on the strain response, nitinol wires were thermally and mechanically treated to create multiple case studies with different phase compositions of wires and thermomechanical loading conditions. For this purpose, constant stress (Fig. 1) and tensile test setups along with an environmental chamber have been used to set different thermomechanical preconditions. Table 1 shows different thermomechanical preconditions on nitinol wires with four different diameters. It should be mentioned that in all cases, the amount of biased stress in heating cycle is lower than the critical stress required for detwinned martensite formation.

The ranges of the critical stresses for formation of detwinned martensite in the cooling cycle have been reported between 80 and 120 MPa for different diameters (Ref 13). In constant stress test setup (Fig. 1), nitinol wire was loaded at a constant level of stress using a weight hanger. The strain response during the thermal cycle was measured by connecting the weight hanger to Linear Variable Differential Transducer (LVDT), a HSD 750-500 manufactured by Macro Sensors. The temperature of nitinol wire was measured with a 0.076-mm Omega K-type thermocouple (Omega Engineering, Stamford, CT, USA) attached to the top portion of the wire. The output signals of both thermocouple and LVDT were collected using SCXI-1321 terminal block (National Instrument, Austin, TX, USA). The same experimental procedure performed by Churchill and Shaw (Ref 34). Nitinol wires have been activated by applying an electrical current produced by a programmable power supply (BK Precision 1696, Yorba Linda, CA, USA) as a step function. An Instron Mini-55 (Artisan Technology Group, Champion, IL, USA) tensile test machine was used with a 10 and 500 N load cell with strain rate of 4×10^{-5} 1/s (displacement control). The test was performed in an isothermal room temperature.

2.2 X-ray Diffraction Test

Nitinol wire segment with the length of 4 cm cut and placed in the goniometer of Bruker Kappa APEX II DUO single-crystal x-ray diffractometer. This equipment is designed for structural determination of single crystal of small molecules.

Table 3 Gaussian's height and position of outstanding peaks for XRD patterns of as-received, cases 1-4 nitinol wires

Thermomechanical case no.	Wire diameter, mm	Major peak height (a), cps	Major peak position (b), (2θ angle)	*R*-square
As-received	0.15	505.70	43.59	0.929
	0.19	615.32	43.53	0.959
	0.24	652.05	43.65	0.937
	0.29	684.09	43.65	0.952
1	0.15	573.55	42.41	0.925
	0.19	1140.00	42.33	0.974
	0.24	599.12	43.63	0.946
	0.29	689.87	43.65	0.997
2	0.15	770.03	42.29	0.964
	0.19	1130.00	42.33	0.979
	0.24	1090.00	42.41	0.955
	0.29	892.17	42.47	0.966
3	0.15	507.68	43.61	0.956
	0.19	477.40	43.49	0.977
	0.24	525.42	43.63	0.969
	0.29	668.76	43.65	0.949
4	0.15	588.01	43.55	0.981
	0.19	526.27	43.47	0.978
	0.24	687.20	43.61	0.974
	0.29	737.68	43.63	0.969

The diffractometer combines a molybdenum x-ray source for high throughput and charge density experiments and a copper source for absolute configuration and protein screening. The x-ray detector is called APEX II, which is basically, a very sensitive CCD (charge couple device) camera covered with phosphor layer. The APEX II software has a graphical user interface that guides the user through the complete experiment and analysis, from data acquisition through data collection, integration, and scaling to structure solution and refinement and report generation. The wires are scanned between 25° and 105°, 2θ angle. The duration of test for scanning the 80° is about 20 min with scanning speed of 4°/min. The size of x-ray beam is about 0.12 mm diameter, which causes some difficulties in scanning the wires with diameter of less than 0.15 mm. To avoid the strain hardening effect at the cutting locations of the wires, the midpoint of the cut wire segment was selected to be scanned by the x-ray beam. The CuKα of 100 kV and 10 mA has been used as x-ray source in this study. MATLAB software was used to analyze the XRD results by performing Gaussian curve fitting analysis. 8 Gaussian curves were applied to each x-ray pattern (n = 8) to detect all possible position and intensity of outstanding peaks in XRD pattern.

$$f(x) = \sum_{i=1}^{n} a \exp\left(-\frac{(x-b)^2}{2c^2}\right).$$

The Gaussian graph is a characteristic symmetric "bell curve" shape. The parameters a, b, and c represent the peak's height, position, and the width of the peak, respectively. A curve fitting with *R*-square value equal and greater than 0.98 has been resulted for all XRD patterns of different wire diameters at different thermomechanical cases. To eliminate or minimize the noises produced by machine, we ran the test without any nitinol wires in sample holder and then subtract this pattern from the patterns resulted from nitinol wires.

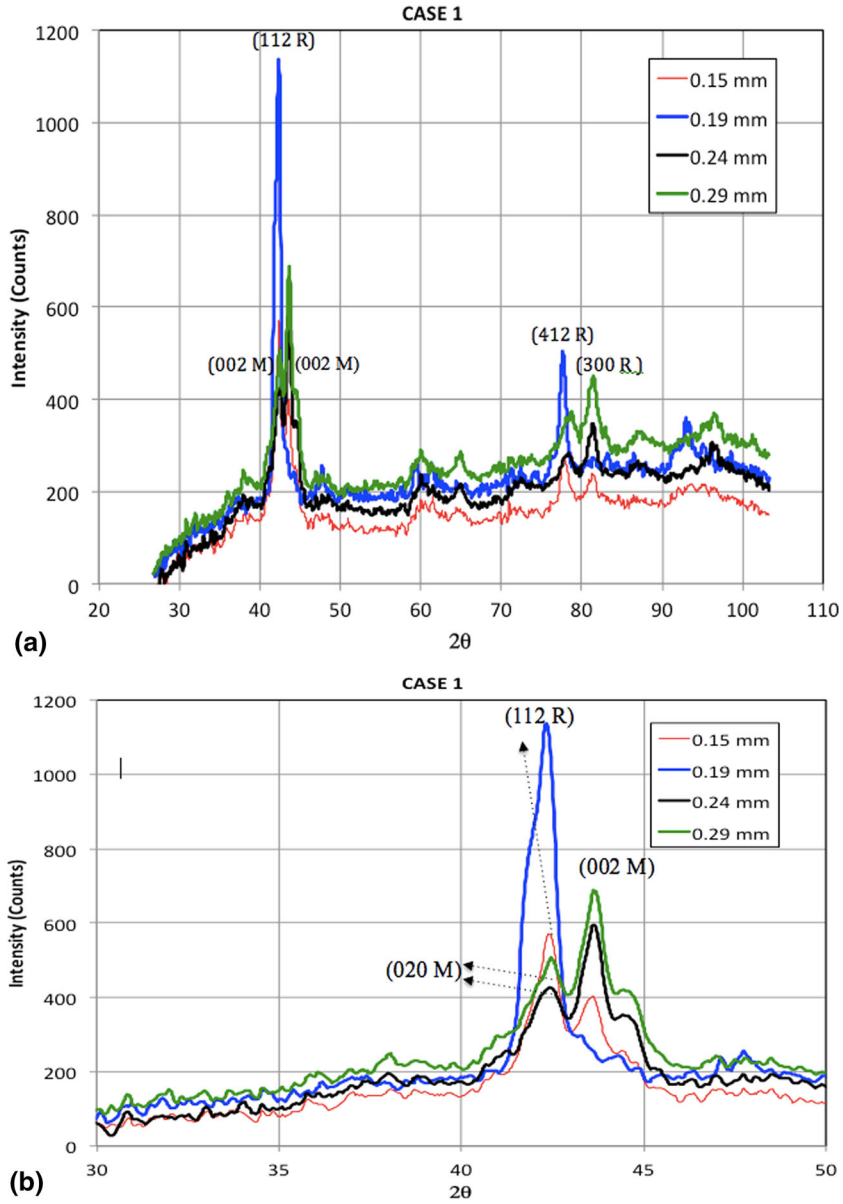

Fig. 5 (a) Complete XRD pattern of Case 1 wires; (b) XRD patterns between 30° and 50° 2θ angle

In this study, the detection of phases is based on large, outstanding peak at the 2θ angle of 40° to 45°. The portion of each XRD pattern that is located between 2θ angle of 35° and 50° was plotted separately in each case for comparison of phase composition in different wire diameters. All XRD tests have performed at room temperature for all wire diameters in different preconditioning cases.

3. Results and Discussion

3.1 Variation of Nitinol Microstructure During Thermomechanical Cycle

The transformation temperatures of the wires were first measured using DSC. The results are presented in Table 2 and Fig. 2. These results were used to predict the generated phase composition after each conditioning step. According to Table 2, heating the wire in the range of 70-80 °C has to be high enough to transform the detwinned martensite phase state (as-received condition) to austenite. A cooling cycle to room temperature (22-25 °C) caused the formation of R-phase, i.e., intermediate phase between austenite and martensite, from austenite. This phase was formed since the temperature did not go low enough to reach M_s. In order to eliminate the R-phase, wires were cooled in a cooling chamber to −40 °C where the martensite phase was formed.

Honarvar et al. (Ref 13) found the difference in macroscopic mechanical strain response of nitinol wires with diameter less than 0.19 mm and larger than 0.19 mm. Based on their observations, the amount of unrecovered strain in diameters of less than 0.19 mm was high while the stress level was less than the range of critical stress while heated to 70-80 °C and cooled back to the room temperature. This dependency to the amount of biased stress has not been observed in the wire diameters larger than 0.19 mm. Figure 3(a) and (b) demon-

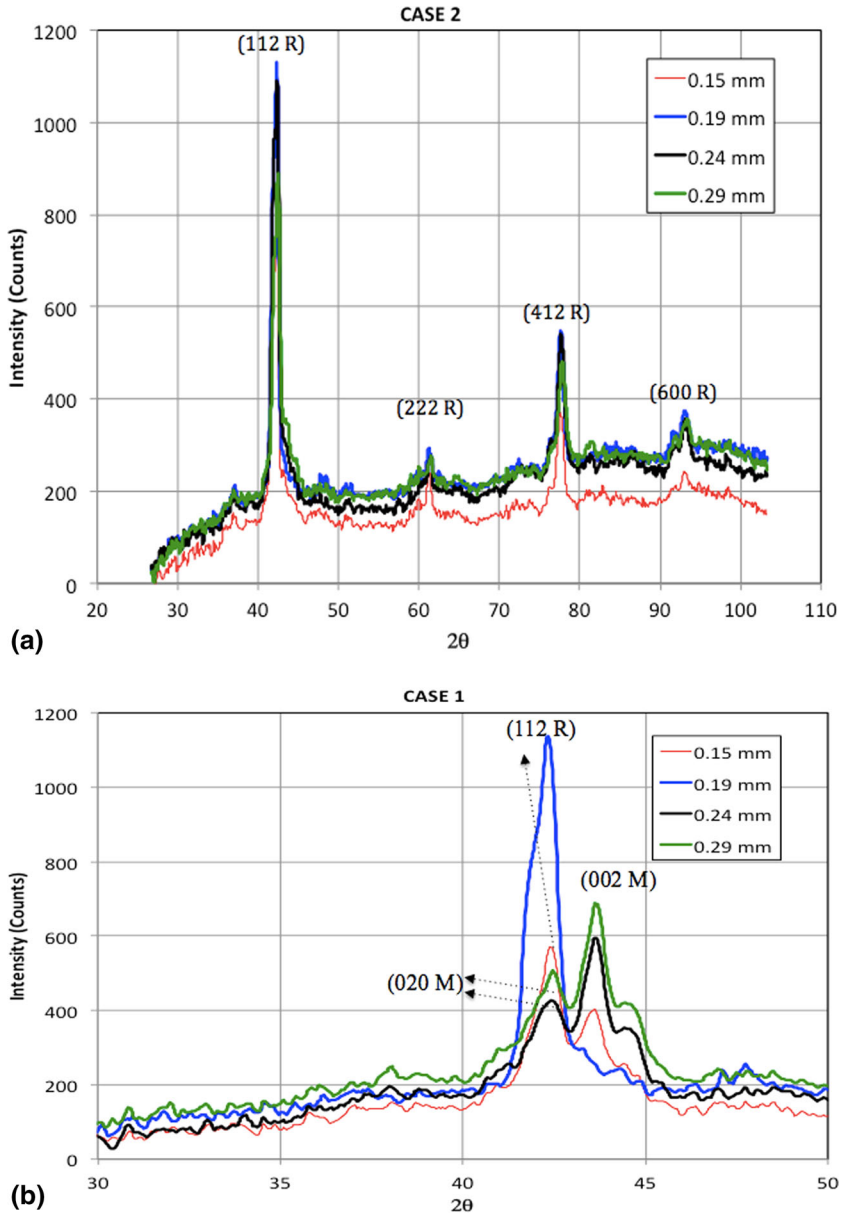

Fig. 6 (a) Complete XRD pattern of Case 2 wires; (b) XRD patterns between 30° and 50° 2θ angle

strates the unrecovered strain of one-way shape memory nitinol of four different diameters. They have reported the unrecovered strain to be about 4% for the diameters of 0.15 and 0.19 mm. This amount of unrecovered strain caused a negligible strain in the next thermal cycle. On the other hand, the unrecovered strain for diameters of 0.24 and 0.29 mm has been reported about 0.5%. This discrepancy was confirmed by capturing the microstructure of the wires after each thermomechanical loading.

Figure 3(a) and (b) illustrates the difference in strain response of nitinol wires for diameters less than 0.19 mm and larger than 0.19 mm as they were treated with the same thermomechanical condition of Case 1. These results were achieved by performing constant stress experiment at case 1 thermomechanical condition with different biased stresses on different wire diameters. As seen in Fig. 3(a), unrecovered strain is huge (about 4%) for diameters of 0.15 and 0.19 mm while the unrecovered strain is negligible (about 0.5%) for diameters of 0.24 and 0.29 mm at the heating range of 70-80 °C (Case 1). The squares and circles show the abstract value of experimental results where the straight and dashed lines demonstrate the best linier fitting pass through the points. There are two kinks in plots of wire diameters less than 0.19 mm which considered as starting and finishing critical stresses at the heating range of 70-80 °C (Ref 13). In order to understand the reason of this difference between two groups of wires, the phase compositions of these wires while subjected to the thermomechanical loadings were investigated.

Figure 4(a) shows the whole XRD pattern of four diameters of as-received wires between 25° and 105° (2θ). The XRD patterns of as-received wires showed that these wires have the same phase state of detwinned martensite. Figure 4(b) shows

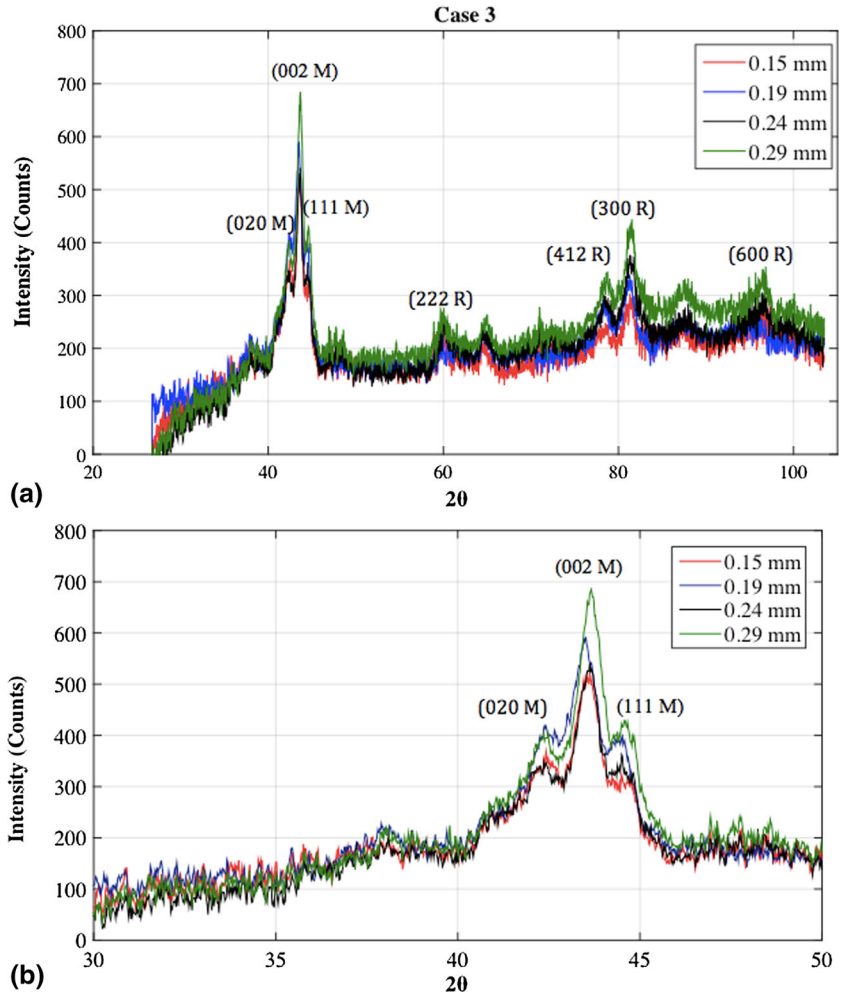

Fig. 7 (a) Complete XRD pattern of Case 3 wires; (b) XRD patterns between 30° and 50° 2θ angle

characteristic peaks in the range of 35°-50° (2θ) since detection of different phases occurs between 40° and 45° (2θ).

Table 3 illustrates the values for a and b and parameters of Gaussian curve fitting for Fig. 4(b). The decrease in intensity of peak (a) in 0.15 mm can be related to small diameter of the wire compared to the size of x-ray beam (0.12 mm), which causes lower reflection. From Fig. 4 and Table 3, it can be concluded that all four as-received diameters have the same phase composition of detwinned martensite. In comparison to the other studies (Ref 24-33), it can be concluded that the major part of initial existed phase in all four wire diameters are detwinned martensite with peaks at the 2θ angle of 43.5, which is the characteristic peak of martensite phase.

Case 1 preconditioning was applied in investigating the strain behavior of Nitinol wires of various sizes subjected to thermal cycle of 70-80 °C. As mentioned above, the macroscopic strain response of all wires was divided into two categories (wire diameters smaller and larger than 0.19 mm). Figure 5 shows the XRD patterns of the nitinol wires after preconditioning for Case 1. Figure 5(a) shows the whole XRD pattern of four diameters between 25° and 105° (2θ). Figure 5(b) demonstrates the XRD patterns between 35° and 50° (2θ) of 0.15, 0.19, 0.24, and 0.29 mm wire diameters, respectively. Table 3 illustrates the values for a and b, parameters of Gaussian curve fitting for Fig. 5(b).

The detection of dominant phase in each diameter is based on the highest peak intensity observed in XRD pattern. As it is presented in Fig. 5 and Table 3, XRD patterns for diameters of 0.15 and 0.19 mm are different from 0.24 and 0.29 mm. The generated phase state for the diameters less than 0.19 mm after Case 1 treating condition is R-phase with outstanding peak occurring at the 2θ angle around 42.3° while the detwinned martensite occurs at 2θ angle of 43.6° for diameters of 0.24 and 0.29 mm. For 0.15 mm, although both peaks of (112 R) and (002 M) are observed at 2θ angle of 42.41 and 43.36, respectively, the intensity of (112 R), 573.55 cps, is more than the peaks of (002 M), 400 cps. Consequently, it can be concluded that the dominant phase composition at wire diameter of 0.15 mm is R-phase although considerable amount of Martensite is also presented. This difference in phase state can justify the difference in the amount of unrecovered strain demonstrated in Fig. 3. The reason for such behavior can be the insufficient heating for transforming the phase state from detwinned martensite to austenite during heating in diameters of 0.24 and 0.29 mm at the heating range of 70-80 °C. Consequently, the major portion of phase state for these diameters is untransformed and intact detwinned martensite.

It has been showed in Honarvar et al. (Ref 13) studies that wire diameters larger than 0.19 mm, heated in the range of 120-130 °C, show a large amount of unrecovered strain after being

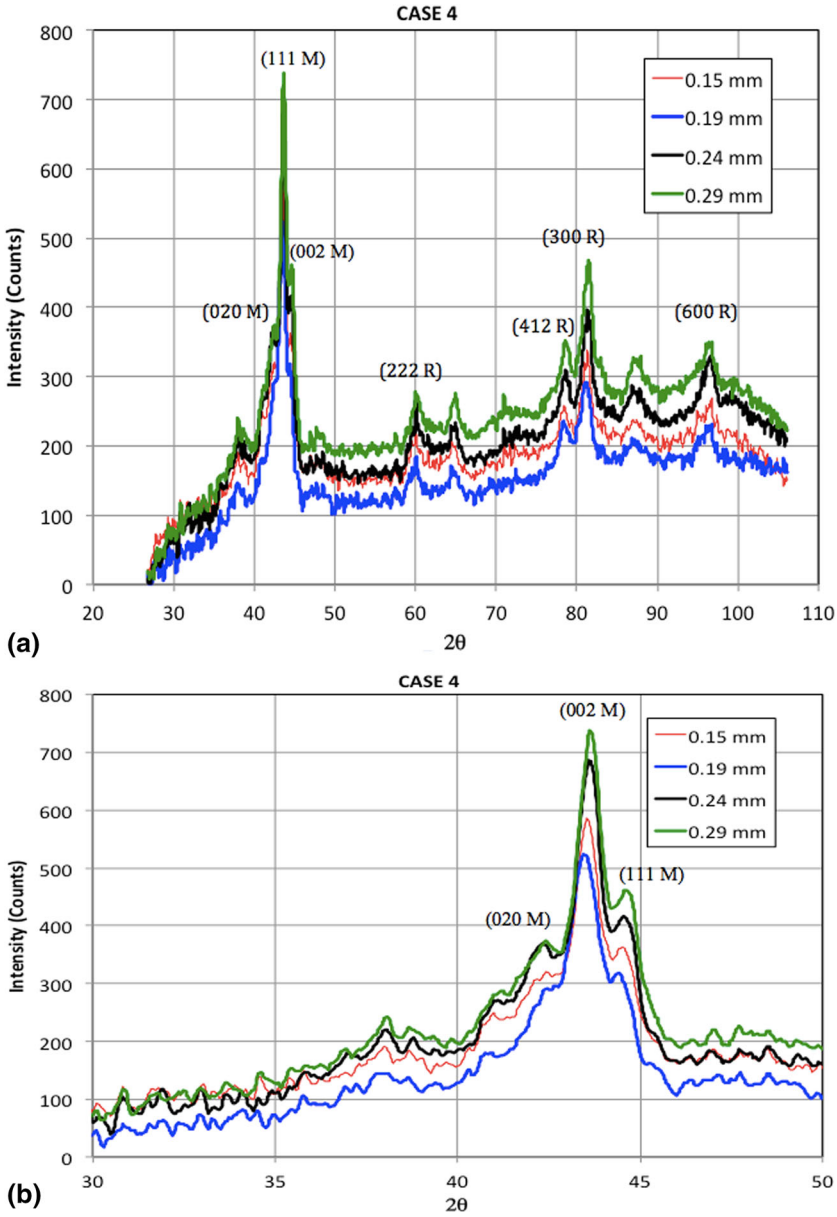

Fig. 8 (a) Complete XRD pattern of Case 4 wires; (b) XRD patterns between 30° and 50° 2θ angle

cooled to room temperature. It was observed that they have the same strain behavior with the wire diameters less than 0.19 mm. To investigate the effect of maximum heating temperature on the strain response of various wire diameters, nitinol wires were treated in Case 2 thermomechanical condition.

The XRD patterns between 25° and 105° (2θ) of nitinol wires treated in this condition are illustrated in Fig. 6. Figure 6(b) demonstrates the XRD patterns between 35° and 50° (2θ). Table 3 shows the values for a and b parameters of Gaussian curve fitting for Fig. 6(b). Figure 6 shows the uniform XRD patterns for all wire diameters while treated in Case 2. From Fig. 6(b), it can be observed that R-phase with characteristic peak occurring at 2θ about 42.3° has been generated in all four nitinol wire diameters where they were heated to 120 to 130 °C and then cooled back to room temperature. R-phase phase state confirms the reason for the formation of high unrecovered strains in all wires where initial phase for all as-received wires is detwinned martensite.

3.2 Microstructural Transformation Between Twinned and Detwinned Martensite

The nitinol wire behavior particularly the transformation of twinned martensite to detwinned martensite has been discussed in Ref 13. Investigating the difference of the phase state of twinned and detwinned martensite, the nitinol wires were treated in Cases 3 and 4, respectively. In Case 3, the nitinol wires treated in Case 1 and have R-phase phase composition at room temperature, were cooled in an environmental chamber to −40 °C, free of stress, to form the twinned martensite phase. In Case 4, the wires thermomechanical conditioned in Case 3 were subjected to tensile stress to reach the 5% strain. This process transforms twinned martensite to detwinned martensite. The

XRD patterns of these wires are shown in Fig. 7 and 8. The XRD pattern illustrated in Fig. 7 shows the twinned martensite phase state with outstanding peak occurring around 43.5° (2θ). Table 3 illustrates a and b parameters of Gaussian curve fitting of Fig. 8(b).

Figure 8(a) shows the XRD pattern of nitinol wires with different diameters treated in Case 4. Figure 8(b) demonstrates the characteristic peak occurring between 35° and 50° (2θ). Table 3 shows a and b parameters of Gaussian curve fitting of Fig. 8(b).

The difference between phase composition of twinned and detwinned martensite in XRD patterns can be emphasized by the difference in intensity of characteristic peak of martensite that occurs at 43.5° (2θ angle). Detwinned martensite has higher XRD peaks intensity. Twin boundaries and disordered surface in the of Twinned Martensite reduce the number of reflected x-ray counts accumulating by x-ray detector from the surface of material.

4. Conclusion

The strain behavior (unrecovered strain) of nitinol wires under the thermal cycle of 70-80 °C was found different for wire diameter less than 0.19 mm (0.15 and 0.19 mm) rather than diameters bigger than 0.19 mm (0.24 and 0.29 mm) where the biased stress during thermal cycle is lower the range of critical stresses (100-140 MPa). For all wire diameters, heated to 120-130 °C, a consistent strain response was reported even in the thermal cycle followed by biased stress lower than the range of critical stress, Fig. 3 and Ref 13. In this paper, phase compositions of the nitinol wires at different thermomechanical conditions were investigated using XRD method. For 0.15 and 0.19 mm diameter wires, heated in the range of 70-80 °C, the R-phase crystal structure was found, while the initial phase was detwinned martensite and therefore stands for the large unrecovered strain.

For 0.24 and 0.29 mm diameter wires, the phase composition was found to be detwinned martensite after they were heated to 70-80 °C. A negligible unrecovered strain was observed for these wire categories. Exposing the wires to a higher temperature in the range of 120-130 °C resulted in formation of R-phase in all wires. Their thermomechanical responses were similar and high unrecovered strains were observed. At the presented diffraction patterns for the samples as-received, only diffraction lines of martensitic phase and possibly weak line of R phase are visible. On the presented diffraction patterns for the samples CASE1, it is clear that they exhibit martensitic phase with a small fraction of R phase whereas in the sample of diameter 0.15 and 0.19 the R-phase is dominant. For case 2, the dominant phase for all the diameters is R-phase. On the presented diffraction patterns for the CASE3 and CASE4, there are clearly visible that martensite is the dominant phase although some fractions of R-phase.

Acknowledgments

The authors would like to acknowledge the contributions of Dr. Michael J. Zdilla and Dr. Fei Ren who are Assistant Professors in the Chemistry and Mechanical Engineering Departments at Temple University. This work is supported by the Department of Defense CDMRP Prostate Cancer Research Program (Grant # W81XWH-11-1-0397/98/99).

References

1. J.A. Shaw, C.B. Churchill, and M.A. Iadicola, Tips and Tricks for Characterizing Shape Memory Alloy Wire: Part 1—Differential Scanning Calorimetry & Basic Phenomena, *Exp. Tech.*, 2008, **32**(5), p 55–62
2. T. Duerig, A. Pelton, and D. Stockel, An Overview of Nitinol Medical Applications, *Mater. Sci. Eng. A*, 1999, **273–275**, p 149–160
3. T.K. Podder, A.P. Dicker, P. Hutapea, and Y. Yu, A Novel Curvilinear Approach for Prostate Seed Implantation, *Med. Phys.*, 2012, **39**, p 1887–1892
4. B. Konh, M. Honarvar, and P. Hutapea, Design Optimization Study of a Shape Memory Alloy Active Needle for Biomedical Applications, *Med. Eng. Phys.*, 2015, **37**(5), p 469–477
5. M. Honarvar, Thermomechanical Characterization of One-Way Shape Memory Nitinol as an Actuator for Active Surgical Needle. Ph.D. Thesis, 2014, ProQuest Dissertations and Thesis, Publication Number: AAT 3671908; Volume: 76-05(E), Section: B
6. N.V. Datla, B. Konh, M. Honarvar, T.K. Podder, A.P. Dicker, Y. Yu, and P. Hutapea, A Model to Predict Deflection of Bevel-Tipped Active Needle Advancing in Soft Tissue, *Med. Eng. Phys.*, 2014, **36**(3), p 285–293
7. B. Konh, M. Honarvar, and P. Hutapea, Simulation and Experimental Studies of the SMA-Activated Needle Behavior Inside the Tissue, *Proc. SPIE 9431, Active and Passive Smart Structures and Integrated Systems 2015*, Mar 2015 (San Diego, CA)
8. B. Konh, M. Honarvar, and P. Hutapea, Application of SMA Wire for an Active Steerable Cannula, *ASME Conference on Smart Materials, Adaptive Structures and Intelligent Systems*, Sep 2013 (Snowbird, UT)
9. M. Honarvar, B. Konh, N. V. Datla, S. Devlin, and P. Hutapea, Size Effect on the Critical Stress of Nitinol Wires, *ASME Conference on Smart Materials, Adaptive Structures and Intelligent Systems*, Sep 2013 (Snowbird, UT)
10. N. V. Datla, M. Honarvar, T. M. Nguyen, B. Konh, K. Darvish, Y. Yu, A. P. Dicker, T. K. Podder, and P. Hutapea, Towards a Nitinol Actuator for an Active Surgical Needle, *ASME Conference on Smart Materials, Adaptive Structures and Intelligent Systems*, Sep 2012 (Stone Mountain, GA)
11. M. Honarvar, B. Konh, and P. Hutapea, Investigation of Crystal Structures of One-Way Shape Memory Nitinol Wire Actuators for Active Steerable Needle, *Proc. SPIE 9432, Behavior and Mechanics of Multifunctional Materials and Composites 2015*, Mar 2015 (San Diego, CA)
12. D.C. Lagoudas, *Shape Memory Alloys Modeling and Engineering Applications, Chapter 2*, Springer, New York, 2008, p 64–75
13. M. Honarvar, N.V. Datla, B. Konh, T.K. Podder, A. Dicker, Y. Yu, and P. Hutapea, Study of Unrecovered Strain and Critical Stresses in One-Way Shape Memory Nitinol, *J. Mater. Eng. Perform.*, 2014, **23**(8), p 2885–2893
14. S. Leclercq and C. Lexcellent, A General Macroscopic Description of the Thermomechanical Behavior of Shape Memory Alloys, *J. Mech. Phys. Solids*, 1996, **44**(6), p 953–980
15. Y. Liu and Z. Xie, Detwinning in Shape Memory Alloy, *Progress in Smart Materials and Structures, Chapter 3*, P.L. Recee, Ed., Nova Science Publishers Inc, Singapore, 2007, p 29–65
16. Y. Liu, Z. Xie, J.V. Humbeeck, L. Delaey, and Y. Liu, On the Deformation of the Twinned Domain in NiTi Shape Memory Alloys, *Philos. Mag. A*, 2000, **80**(8), p 1935–1953
17. A. Saigal and M. Fonte, Solid, Shape Recovered Bulk Nitinol: Part I—Tension-Compression Asymmetry, *Mater. Sci. Eng. A*, 2011, **528**, p 5536–5550
18. J.A. Shaw, C.B. Churchill, and M.A. Iadicola, Tips and Tricks for Characterizing Shape Memory Alloy Wire: Part II—Fundamental Isothermal Response, *Exp. Tech.*, 2009, **33**(1), p 51–62
19. J.G. Boyd and D.C. Lagoudas, A Thermodynamical Constitutive Model for Shape Memory Materials. Part I. The Monolithic Shape Memory Alloy, *Int. J. Plast.*, 1996, **12**(6), p 805–842
20. G. Costanza, M.E. Tata, and C. Calisti, Nitinol One-Way Shape Memory Springs: Thermomechanical Characterization and Actuator Design, *Sens. Actuators A*, 2010, **157**, p 113–117

21. D.C. Lagoudas and S.G. Shu, Residual Deformation of Active Structures with SMA Actuators, *Int. J. Mech. Sci.*, 1999, **41**(6), p 595–619
22. L.C. Brinson, One-Dimensional Constitutive Behavior of Shape Memory Alloys: Thermomechanical Derivation with Non-constant Material Functions and Redefined Martensite Internal Variable, *J. Intell. Mater. Syst. Struct.*, 1993, **4**(2), p 229–242
23. J.M. San Juan, M.L. No, and C.A. Schuh, Superelasticity and Shape Memory in Micro- and Nanometer-Scale Pillars, *Adv. Mater.*, 2008, **20**, p 272–278
24. M. Iijima, W.A. Brantley, W.H. Guo, W.A.T. Clark, T. Yuasa, and I. Mizoguchi, X-ray Diffraction Study of Low-Temperature Phase Transformations in Nickel-Titanium Orthodontic Wires, *Dent. Mater.*, 2008, **24**, p 1454–1460
25. T.A. Thayer, M.D. Bagby, R.N. Moore, and R.J. DeAngelis, X-ray Diffraction of Nitinol Orthodontic Arch Wires, *Am. J. Orthod. Dentofacial Orthop.*, 1995, **107**(6), p 604–612
26. M. Iijima, H. Ohno, I. Kawashima, K. Endo, W.A. Brantley, and I. Mizoguchi, Micro X-ray Diffraction Study of Superelastic Nickel-Titanium Orthodontic Wires at Different Temperatures and Stresses, *Biomaterials*, 2002, **23**, p 1769–1774
27. M. Iijima, W.A. Brantley, I. Kawashima, H. Ohno, W. Guo, Y. Yonekura, and I. Mizoguchi, Micro-X-ray Diffraction Observation of Nickel-Titanium Orthodontic Wires in Simulated Oral Environment, *Biomaterials*, 2004, **25**, p 171–176
28. S. Kheir, W. Brantley, and R. Fournelle, Structure Characterization of Superelastic NiTi Orthodontic Wires Alloys, *J. Dental Res.*, 1988, **67**, p 361
29. S. Kheir, W. Brantley, R. Fournelle, and T. Ehlert, XRD and DSC Studies of NiTi Orthodontic Wire Alloys, *J. Dental Res.*, 1989, **68**, p 386
30. S. Cai, J.E. Schaffer, Y. Ren, and C. Yu, Texture Evolution During Nitinol Martensite Detwinning and Phase Transformation, *Appl. Phys. Lett.*, 2013, **103**(24), p 241909
31. Y. Shen, H. Zhou, Y. Zheng, B. Peng, and M. Haapasalo, Metallurgical Characterization of Controlled Memory Wire Nickel-Titanium Rotary Instrument, *Basic Res. Technol.*, 2011, **37**(11), p 1566–1571
32. M. Iijima, H. Ohno, I. Kawashima, K. Endo, and I. Mizoguchi, Mechanical Behavior at Different Temperatures and Stresses for Superelastic Nickel-Titanuim Orthodontic Wires Having Different Transformation Temperatures, *Dent. Mater.*, 2002, **18**, p 88–93
33. S.E. Kheir, W.A. Brantley, and R.A. Fournelle, Structure and Mechanical Properties of As-Received and Heat-Treated Stainless Steel Orthodontic Wires, *Am. J. Orthod. Dentofac. Orthop.*, 1988, **93**, p 206–212
34. C. B. Churchil, J. A. Shaw, Shakedown Response of Conditioned Shape Memory Alloy Wire, *SPIE 6929, Behavior and Mechanics of Multifunctional and Composite Materials*, M. J. Dapino, Z. Ounaies, Eds., San Diego, CA, 2008, 6928